Pop-in Behavior during Nano-indentation on Steel Alloys

Prof. H. N. Han

Seoul National University

(hnhan@snu.ac.kr)

2013.7.24, APMS

Acknowledgements:

Basic Science Research Program through NRF funded by the Ministry of Science, ICT and Future Planning (2013008806) and POSCO (2013Z029)

Collaboration with…

Dr. Tae-Hong Ahn,	*Korea Atomic Energy Research Institute*
Dr. Tae-Ho Lee,	*Korea Institute of Materials Science (KIMS)*
Dr. Easo P. George,	*Oak Ridge National Laboratory, USA*
Dr. Hongbin Bei,	*Oak Ridge National Laboratory, USA*
Prof. Kyu Hwan Oh	*Seoul National University (SNU)*
Prof. Kyung-Tae Park,	*Hanbat National University*
Dr. Kyooyoung Lee	*POSCO*
Mr. Yanghoo Kim	*Seoul National University (SNU)*

Micromechanical Material Testing

Nanoindentation

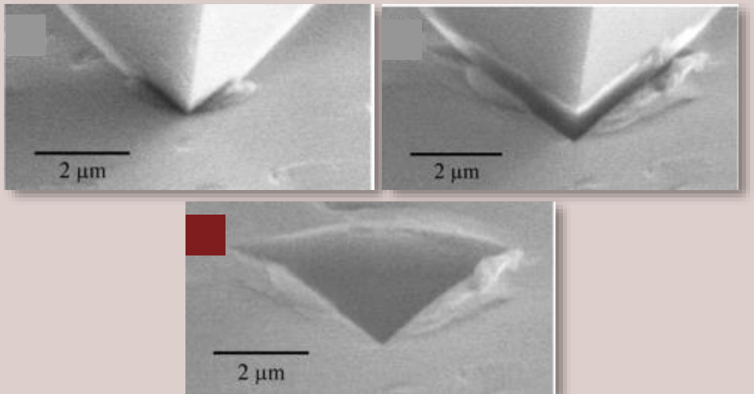

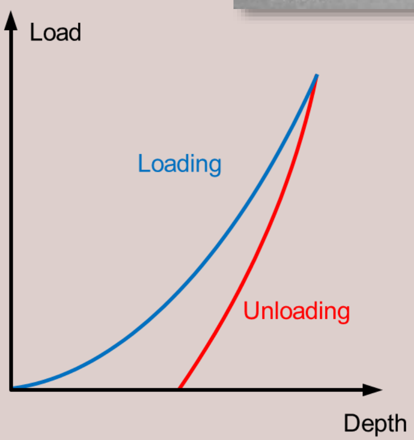

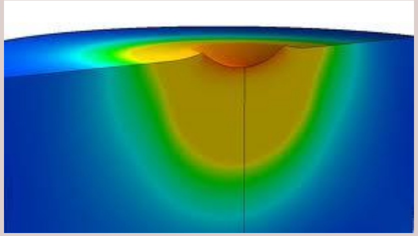

Simple to measure quantitative mechanical properties (hardness, elastic modulus)

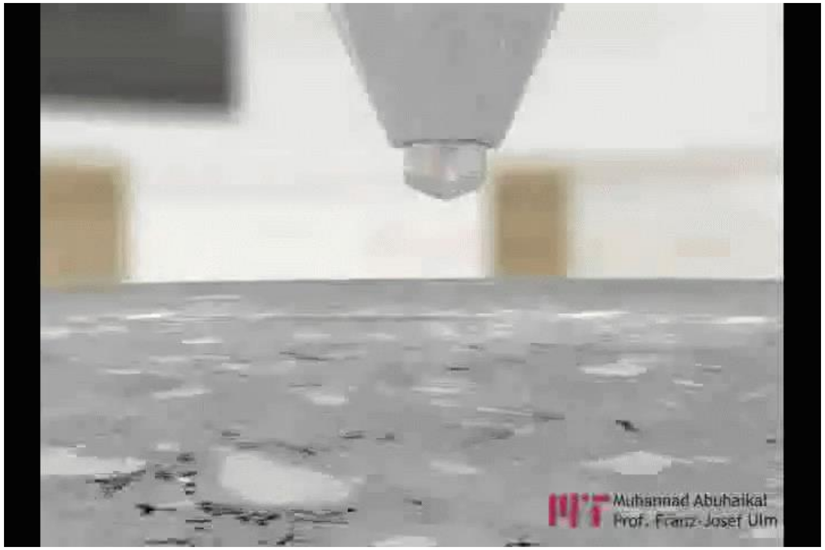

"Nanoindentation video" on YouTube

Indentation Size Effect (ISE)

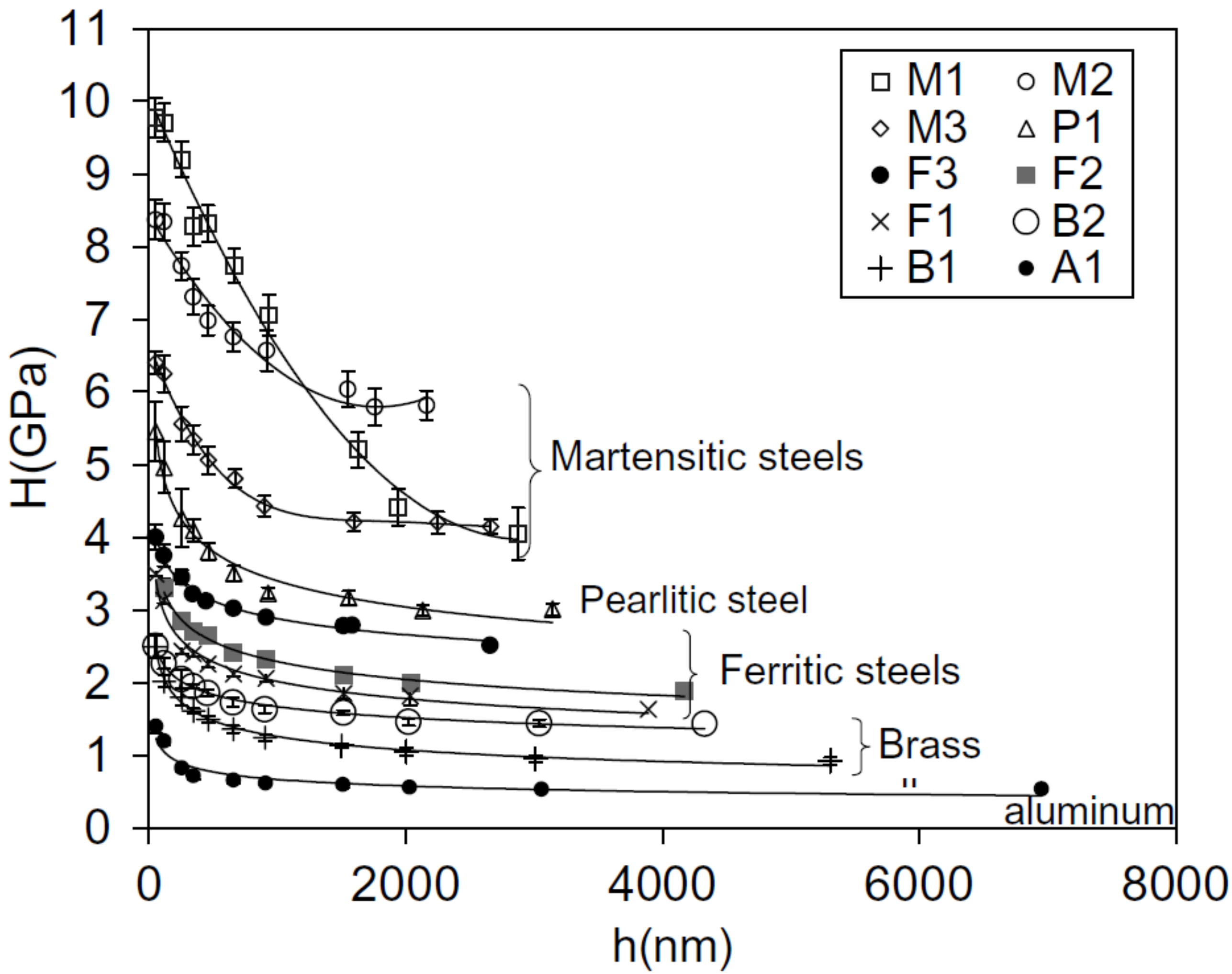

Rodriguez and Gutierrez ; Materials Science and Engineering A (2003)

Probability Effect on Nano-indentation

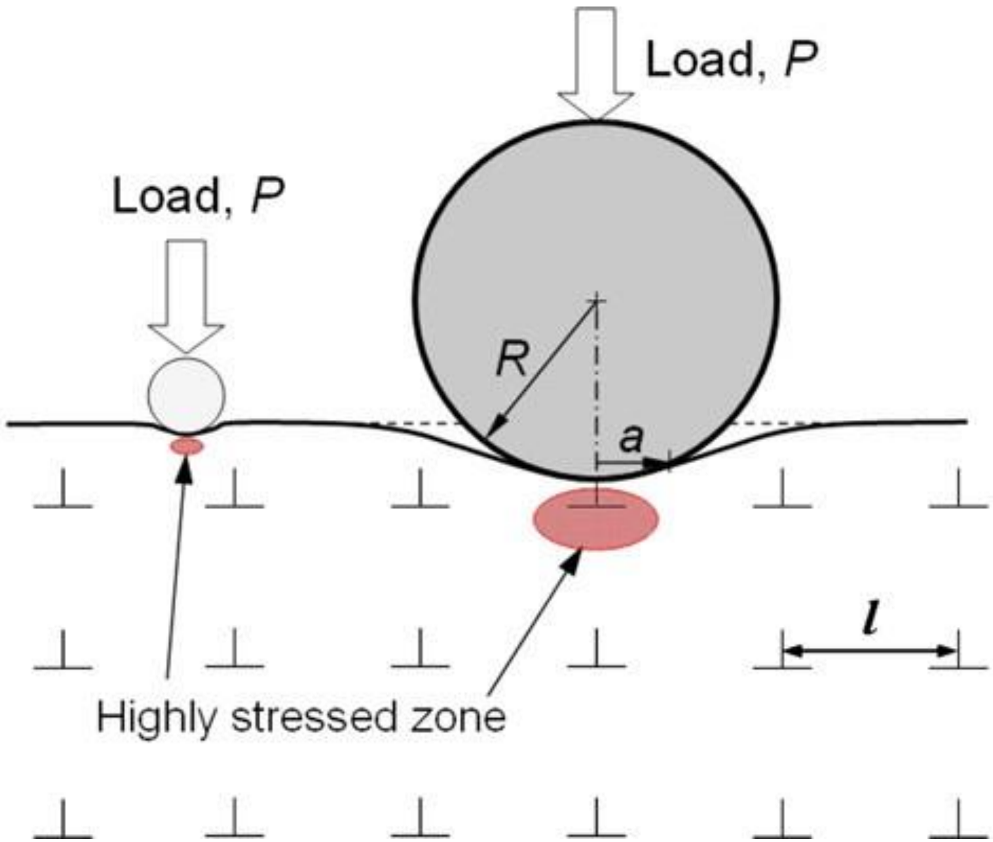

Schematic diagram showing the probability effect by the geometry of the nanoindentation test with spherical indenters.

S. Shim et.al Scripta Materialia (2008)

Nanoindentation Pop-in

L-d curves

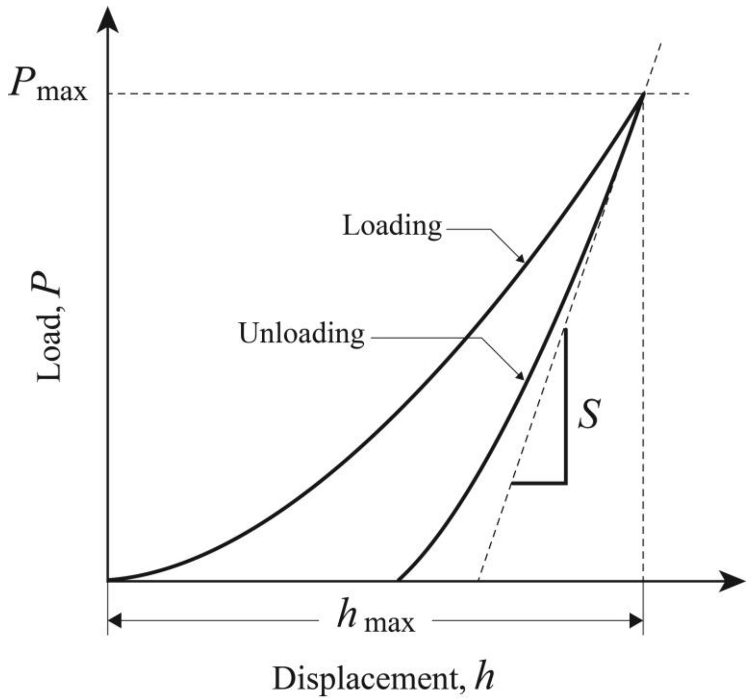

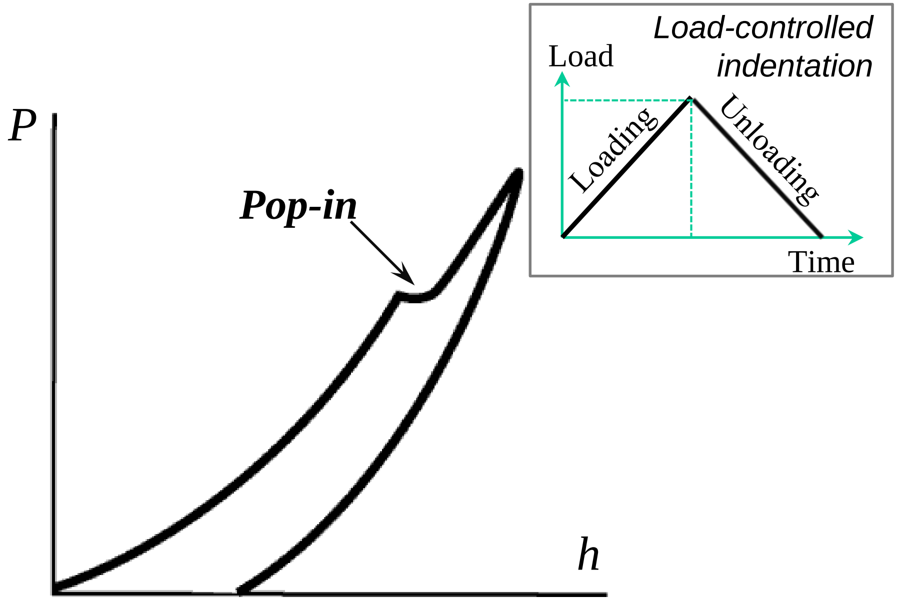

Pop-in

: <u>sudden displacement excursion</u>

Origin of pop-in: Geometrical softening

Nanoindentation Pop-in

The most popular case

: Incipient plasticity

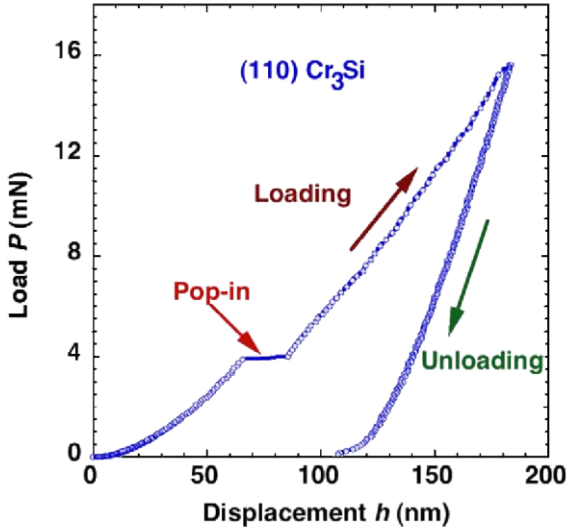

H. Bei et al., Phys. Rev. Lett. (2005)

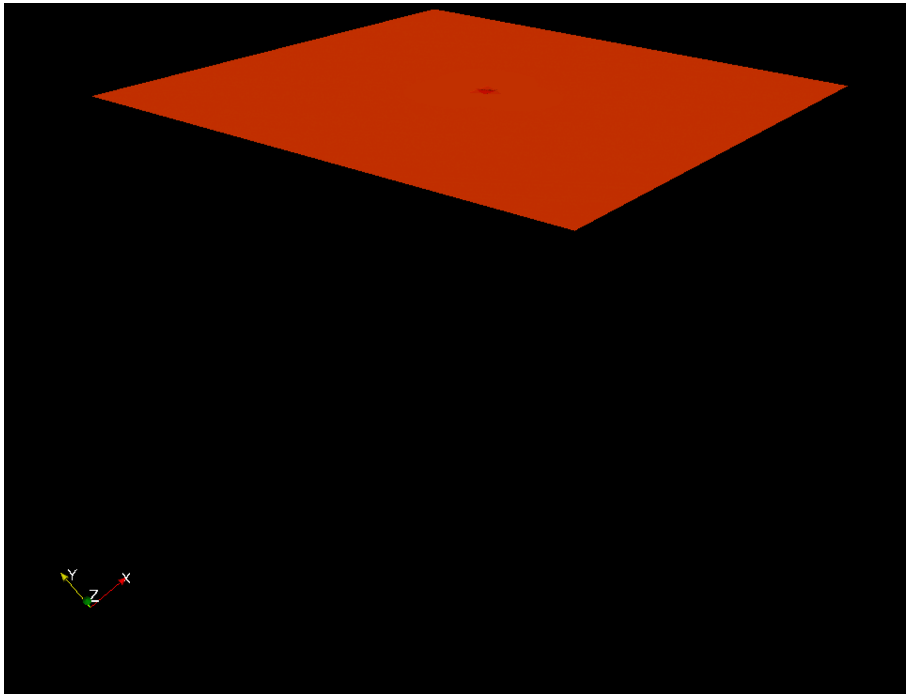

From Dr. Fivel and Dr. Jang in INPG Grenoble

Pop-in occurs as
plastic deformation initiates

**Rough surface, Strained, Large R*
⇒ Less possibility of pop-in

Other sources ?

Possible Sources of Pop-in in Steel

TRIP Steel (α′)

Chemical composition

element	Fe	C	**Mn**	Si	Al
wt.%	bal.	0.08	**7.0**	0.5	1.0

Microstructure

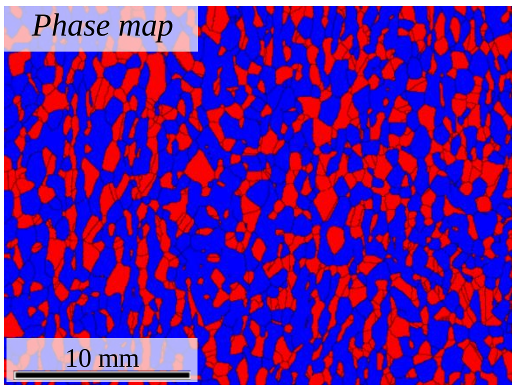

BCC (ferrite, α) FCC (Austenite, γ)

Mechanically induced
γ→α′ transformation

TRIP Steel (ε)

Chemical composition

C	Mn	Si	Ni	**N**	Cr
0.02	5.06	0.19	0.23	**0.28**	20.08

Microstructure

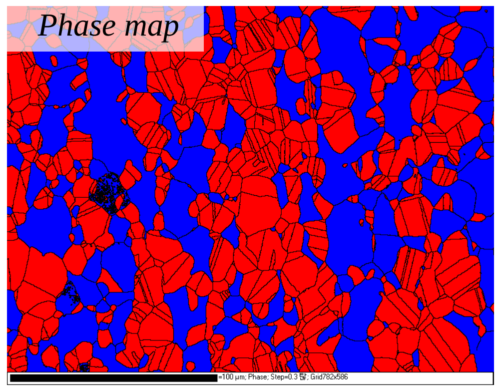

BCC (ferrite) FCC (Austenite)

Mechanically induced
γ→ε transformation

Ferritic Steel

Chemical composition

C	Mn	Si	Al	**N**	Cr
0.06	0.16	0.08	0.02	**0.0006**	0.01

Microstructure

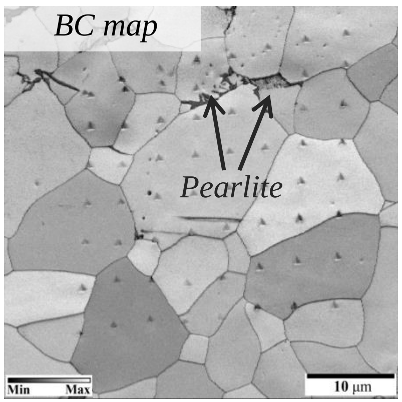

Ferrite : 99% Pearlite : 1%

Sharp yield drop
at yield point

γ→α′ type TRIP steel

Material used

Chemical composition

element	C	Mn	Si	Al	Fe
wt.%	0.08	7.0	0.5	1.0	bal.

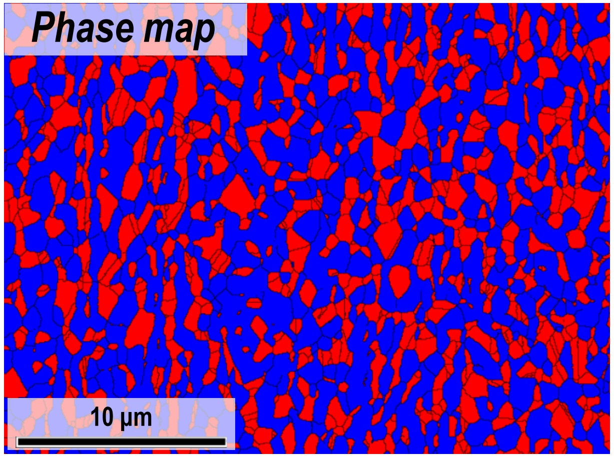

● BCC (ferrite) ● FCC (Austenite)

Volume fraction (%)		
BCC (ferrite)	FCC (austenite)	unindexed (boundaries)
59.7	28.6	11.7

Strain-induced γ(fcc)→α′(bct) transformation occurs

Pop-in Analysis (Austenite)

Nanoindentation

Load-displacement Curve

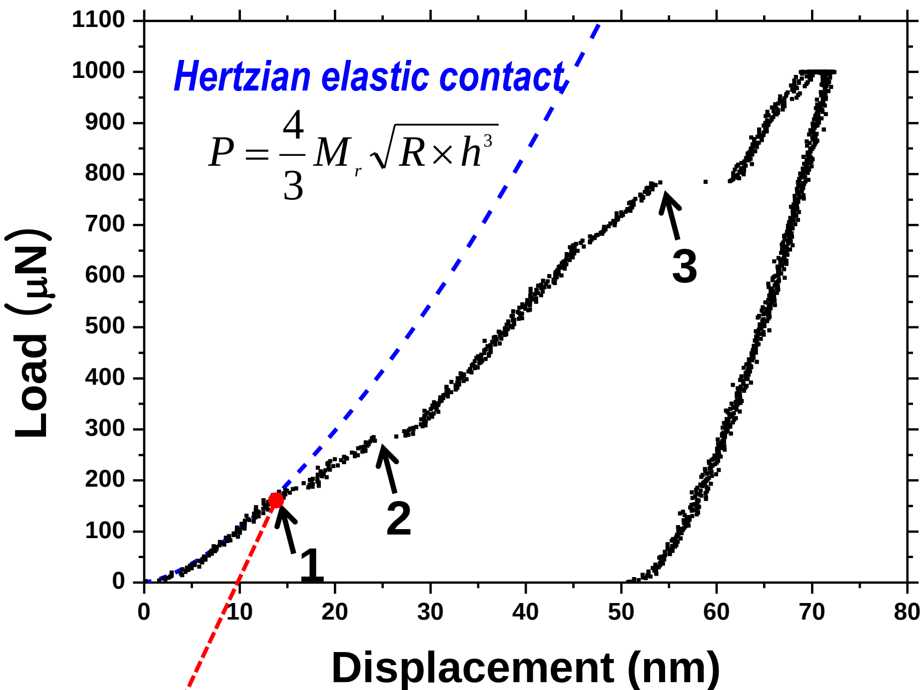

➢ $\tau_m = 0.31\left(\frac{6PE_r^2}{\pi^3 R^2}\right)^{1/3}$ = 9.4 GPa ≒ G/8

: ***τ_m is in the range of the theoretical yield strength***

Indentation Probability Effect

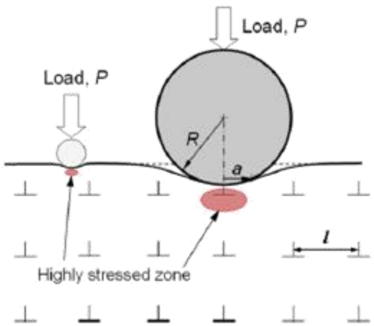

*S. Shim et al., Scripta Mater., 59, 1095 (2008)

Sample History	Dislocation Density ρ (m^{-2})	Mean Distance Between Dislocations (μm)
Annealed	10^{10}	10
Strained	10^{13}-10^{15}	0.1

* Indenter tip radius = **200nm**
* Pop-in (1st) start depth = **15nm**
* Size of the austenite grain = **1.2μm**

The 1st pop-in is likely induced by dislocation nucleation

Pop-in Analysis (Austenite)

Nanoindentation

Load-displacement Curve

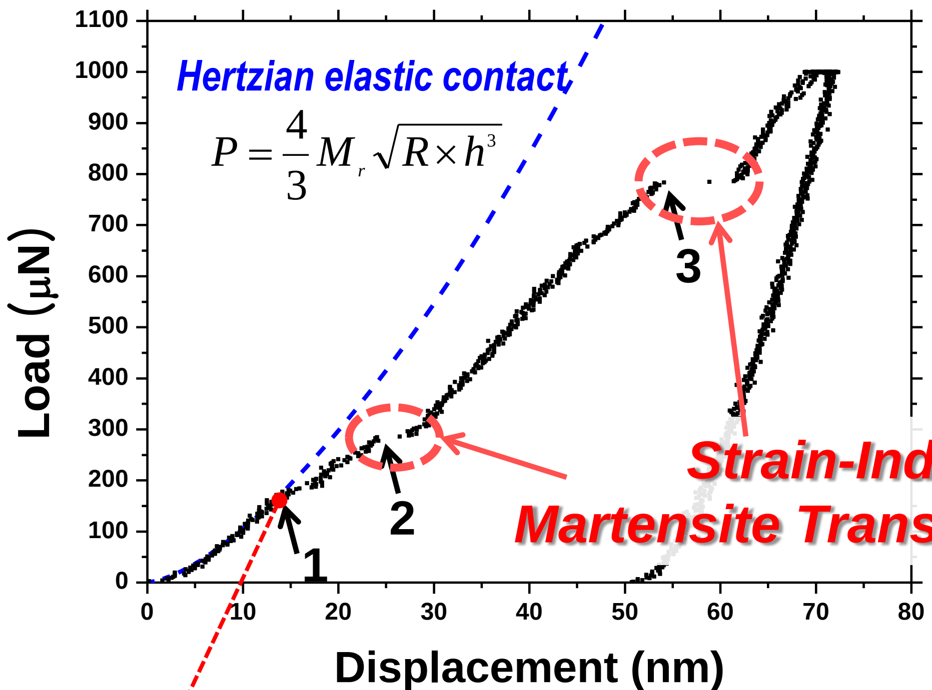

➤ $\tau_m = 0.31\left(\frac{6PE_r^2}{\pi^3 R^2}\right)^{1/3}$ = 9.4 GPa ≒ G/8

: τ_m *is in the range of the* ***theoretical yield strength***

Indentation Probability Effect

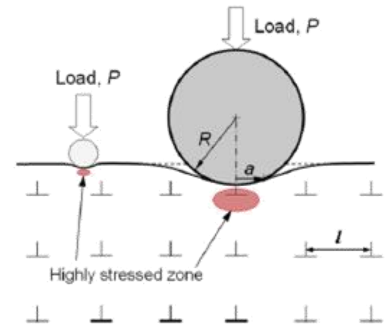

S. Shim et al., Scripta Mater., 59, 1095 (2008)

Sample History	Dislocation Density ρ (m^{-2})	Mean Distance Between Dislocations (μm)
Annealed	10^{10}	10
Strained	10^{13}-10^{15}	0.1

* Indenter tip radius = **200nm**
* Pop-in (1st) start depth = **15nm**
* Size of the austenite grain = **1.2μm**

The 1st pop-in** is likely induced by **dislocation nucleation

TEM Analysis (Austenite)

Cross Section View

*T.-H. Ahn et al., Scripta Mater., 63, 540 (2010)

TEM sampling by FIB

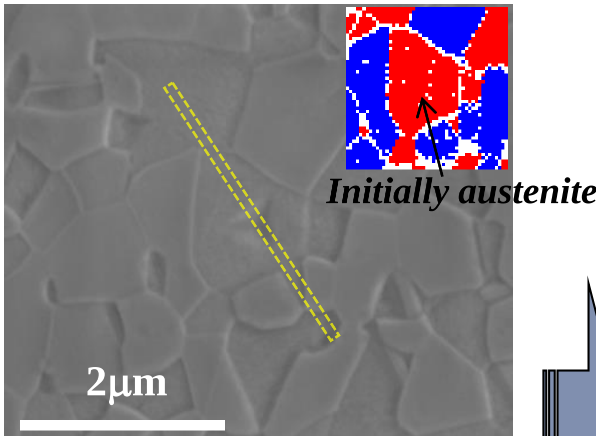

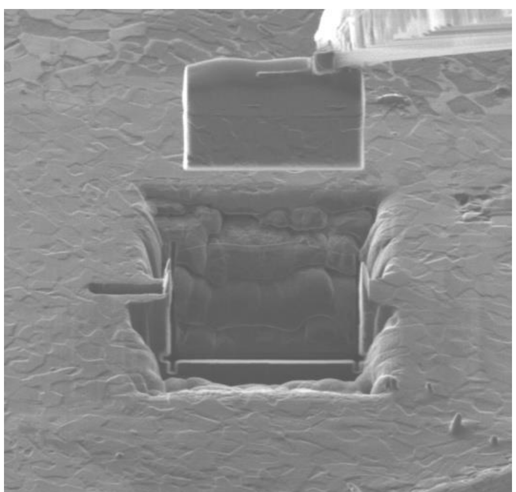

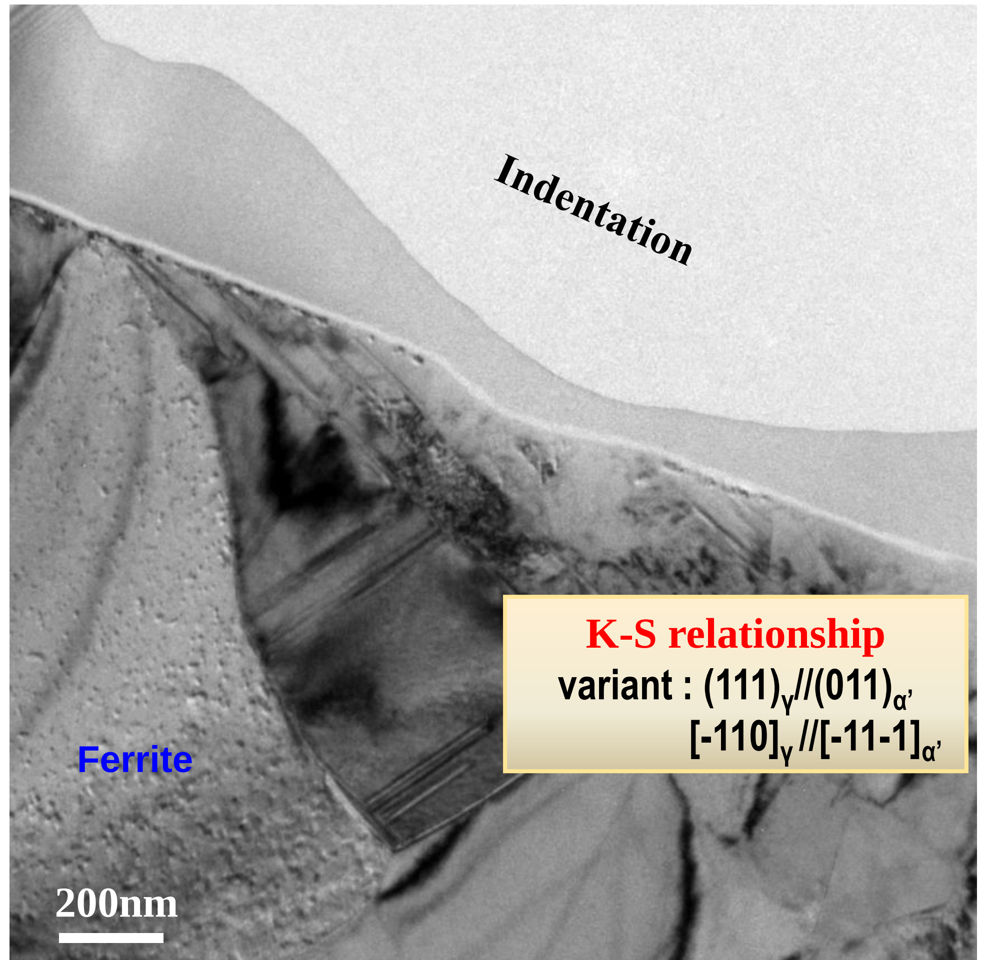

TEM Analysis (Austenite)

Cross Section View

**T.-H. Ahn et al., Scripta Mater., 63, 540 (2010)*

TEM sampling by FIB

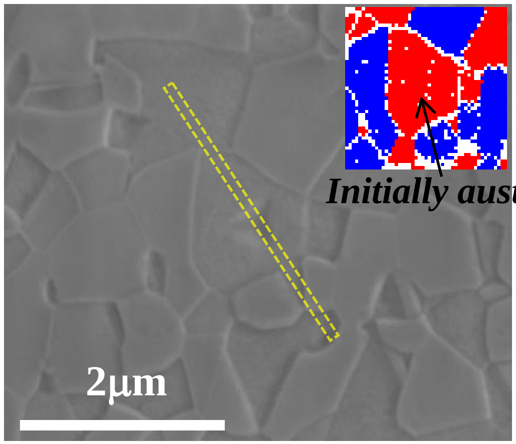

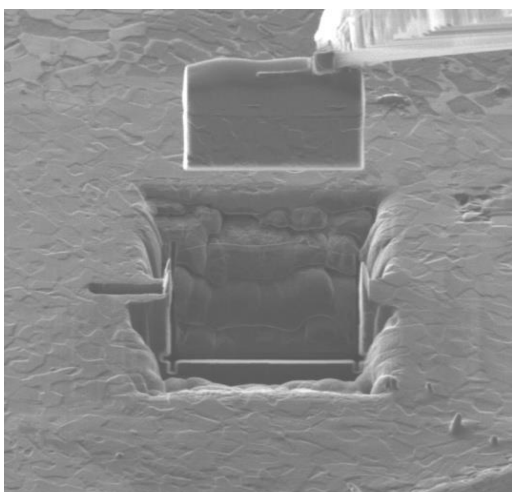

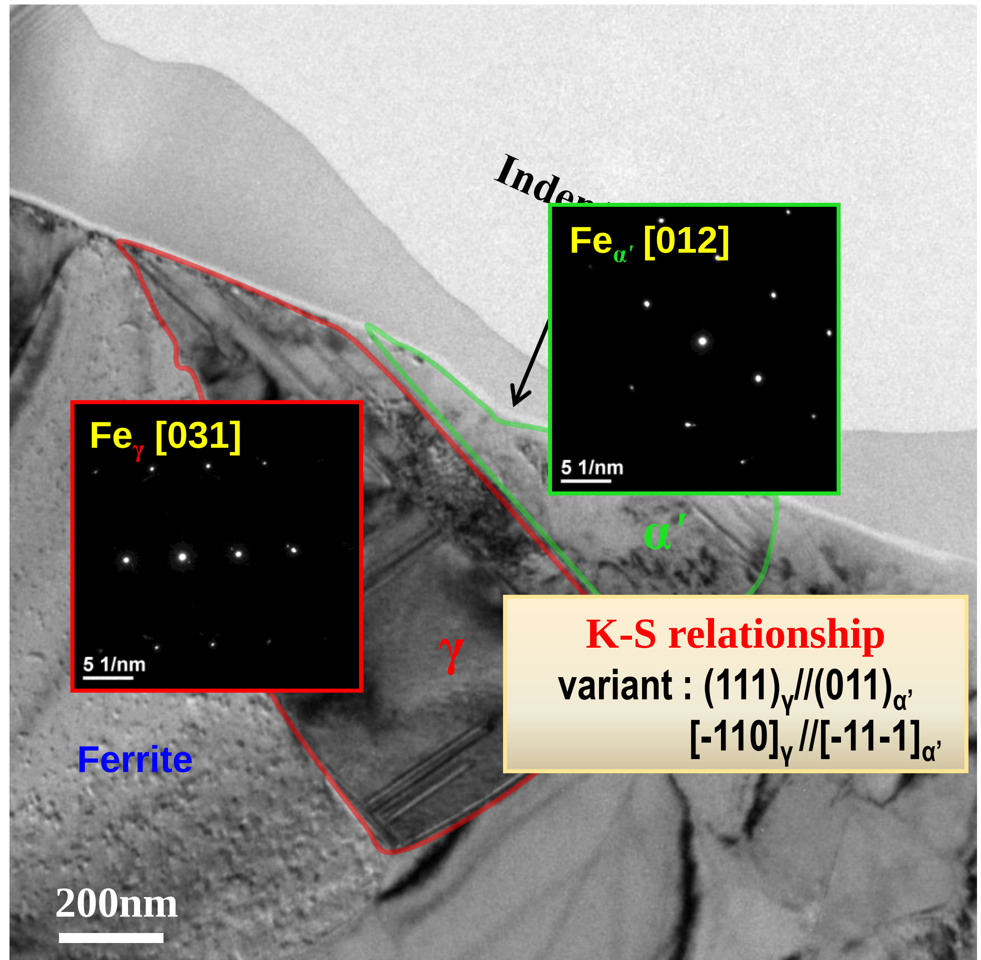

Pop-in Analysis (Austenite)

2nd & 3rd Pop-ins

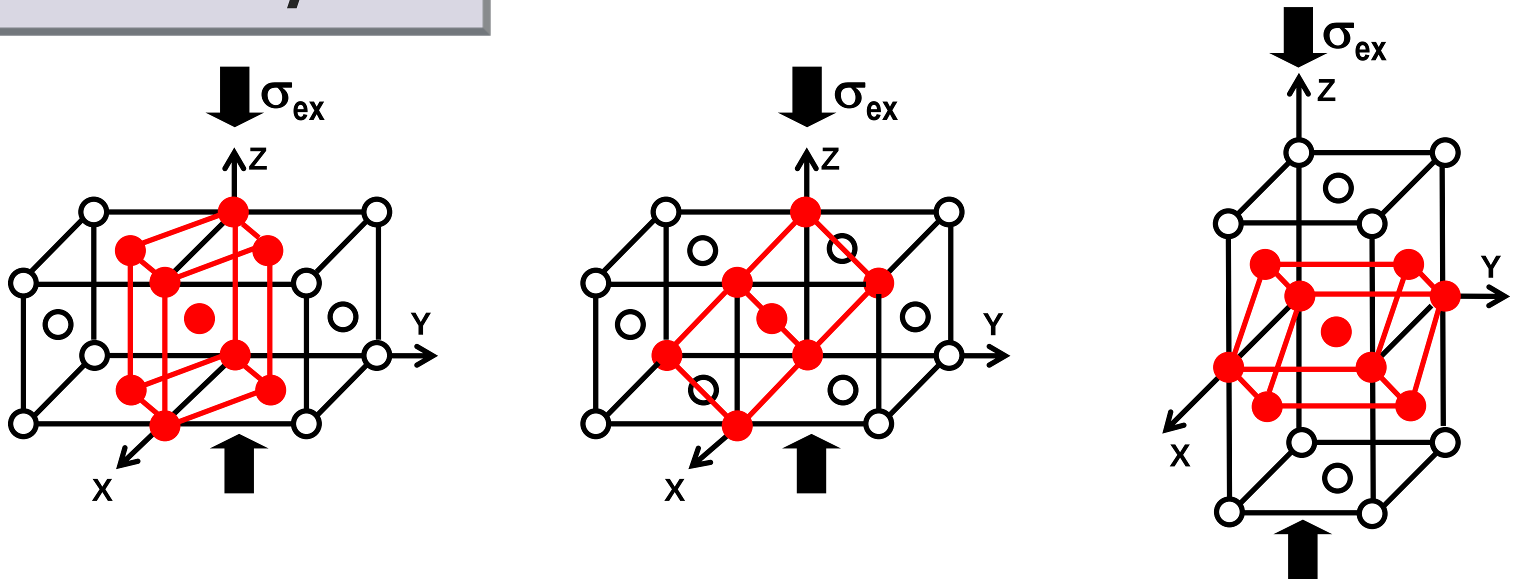

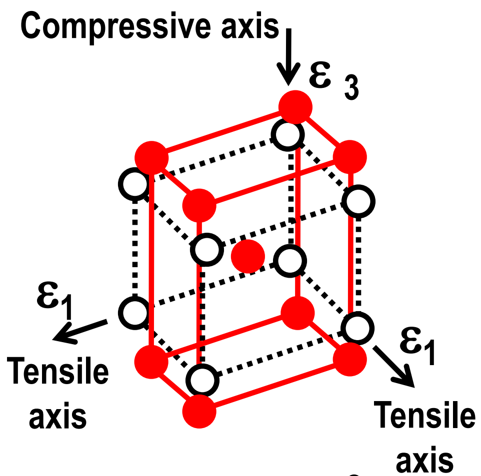

$\varepsilon_1 + \varepsilon_1 + \varepsilon_3 > 0$

Bain Deformation (○ FCC (γ) → ● BCC (α))

- *Stress free, random selection of variant*
  - ➔ *Isotropic volume change*
- *External stress applied*
  - ➔ *Nucleation with particular energetically favorable orientation*
  - ➔ *Anisotropic volume change*

**H.N. Han et al., Acta Mater., 52, 5203 (2004)*

Pop-in Analysis (Austenite)

Pop-in Depth by Martensite Formation

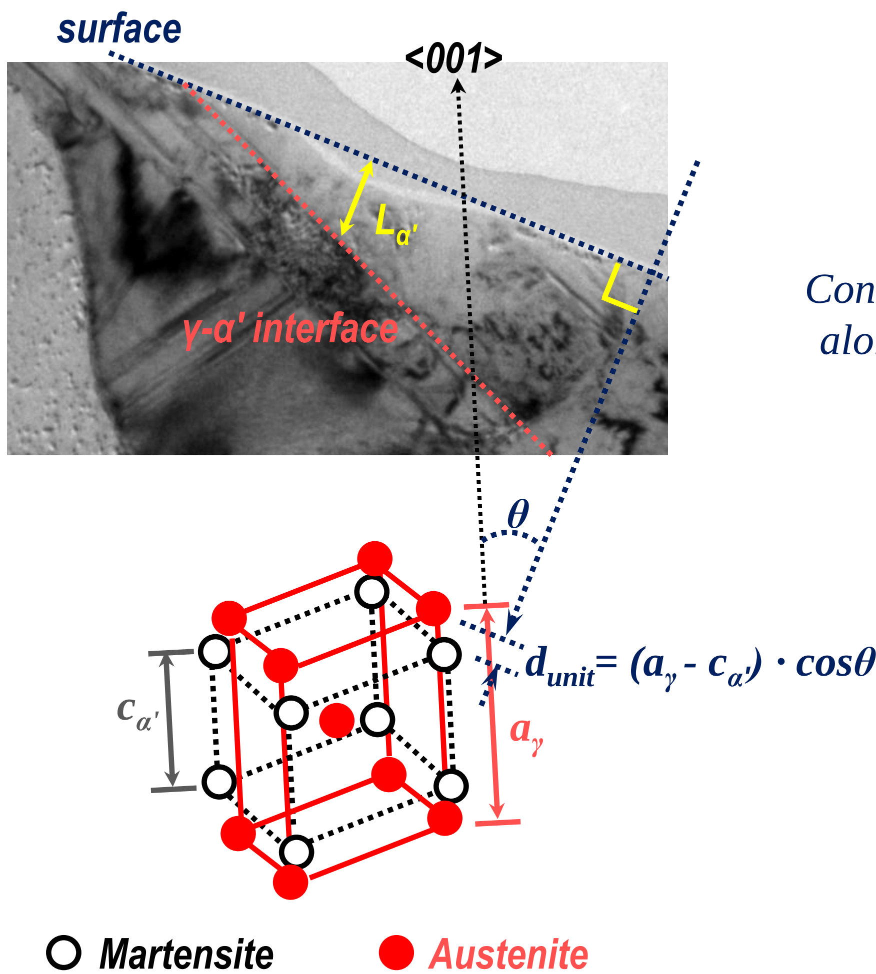

Number of γ unit cells along indentation axis

$$d_{pop-in} = d_{unit} \times \frac{L_{\alpha'}}{a_{\gamma} \cdot \cos\theta}$$

Contraction rate along BCT in γ

$$= \frac{a_{\gamma} - c_{\alpha'}}{a_{\gamma}} \times L_{\alpha'}$$

= 25.2 nm

(≒ 20nm : measured)

- d_{unit} : Amount of pop-in in a unit cell
- $L_{\alpha'}$: Depth of Martensite from the surface
- a_{γ} : Lattice parameter of γ
- $c_{\alpha'}$: c-parameter of Martensite

24 K-S Variants

Variant No.	Plane parallel (γ) // (α)	Direction parallel [γ] // [α]	Variant No.	Plane Parallel (γ) // (α)	Direction Parallel [γ] // [α]
1	(111) // (011)	[-110] // [11-1]	13	(1-11) // (011)	[110] // [11-1]
2	(111) // (011)	[-110] // [-11-1]	14	(1-11) // (011)	[110] // [-11-1]
3	(111) // (011)	[01-1] // [-11-1]	15	(1-11) // (011)	[10-1] // [-11-1]
4	(111) // (011)	[01-1] // [11-1]	16	(1-11) // (011)	[10-1] // [11-1]
5	(111) // (011)	[10-1] // [11-1]	17	(1-11) // (011)	[0-1-1] // [11-1]
6	(111) // (011)	[10-1] // [-11-1]	18	(1-11) // (011)	[0-1-1] // [-11-1]
7	(-111) // (011)	[110] // [11-1]	19	(11-1) // (011)	[-10-1] // [11-1]
8	(-111) // (011)	[110] // [-11-1]	20	(11-1) // (011)	[-10-1] // [-11-1]
9	(-111) // (011)	[01-1] // [-11-1]	21	(11-1) // (011)	[011] // [-11-1]
10	(-111) // (011)	[01-1] // [11-1]	22	(11-1) // (011)	[011] // [11-1]
11	(-111) // (011)	[-10-1] // [11-1]	23	(11-1) // (011)	[1-10] // [11-1]
12	(-111) // (011)	[-10-1] // [-11-1]	24	(11-1) // (011)	[1-10] // [-11-1]

Evaluation of Pop-in

- **Lattice deformation tensor :** $\mathbf{F}_b = \mathbf{B}_b \mathbf{P}_b$

- **Bain deformation tensor (defined on BCC crystal coordinate) :**

$$\eta_3 = \frac{c_{BCT}}{a_{FCC}}, \quad \eta_1 = \frac{\sqrt{2}\, a_{BCT}}{a_{FCC}} \quad \Rightarrow \quad \mathbf{B}_b = \begin{bmatrix} \eta_1 & 0 & 0 \\ 0 & \eta_1 & 0 \\ 0 & 0 & \eta_3 \end{bmatrix}$$

- **Lattice-invariant shear tensor (defined on invariant shear plane) :**

$$\mathbf{P}_i = \begin{bmatrix} 1 & g & 0 \\ 0 & 1 & 0 \\ 0 & 0 & 1 \end{bmatrix}$$

- **Transformation strain tensor (defined on BCC crystal coordinate) :**

$$\varepsilon_{ij}^{C} = \frac{1}{2}[\mathbf{F}_b^{\mathrm{T}} \mathbf{F}_b - \mathbf{I}]$$

Evaluation of Pop-in considering variant selection

$$\varepsilon_{ij}^{C} = \frac{1}{2}[\mathbf{F}^{T}\mathbf{F} - \mathbf{I}]$$

: Transformation strain tensor of 24 variants (crystal coordinates of BCT)

$$\varepsilon_{ij}^{S} = a_{ik} a_{il} \varepsilon_{ij}^{C}$$

: Transformation strain tensor (specimen coordinates)

interaction with external stress due to indentation

$$A^{i} = -\frac{0.011\alpha\delta r (f_{sb})^{r-1}(1 - f_{sb})}{24\Delta S}(\Delta G + \tilde{\sigma}\tilde{\varepsilon}_{S}^{i})$$

: nucleation rate of each variant

Pop-in Analysis

Multiple Pop-ins

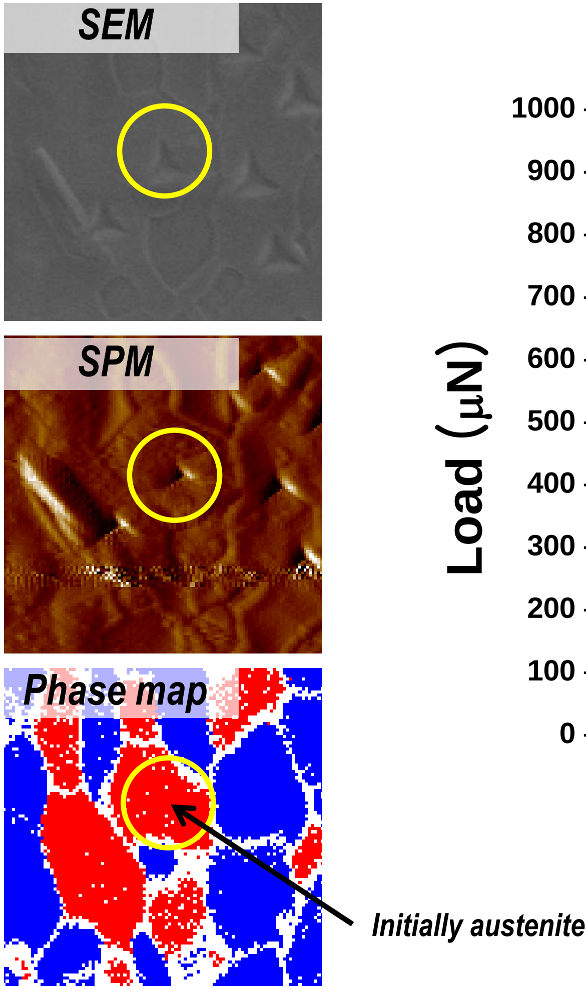

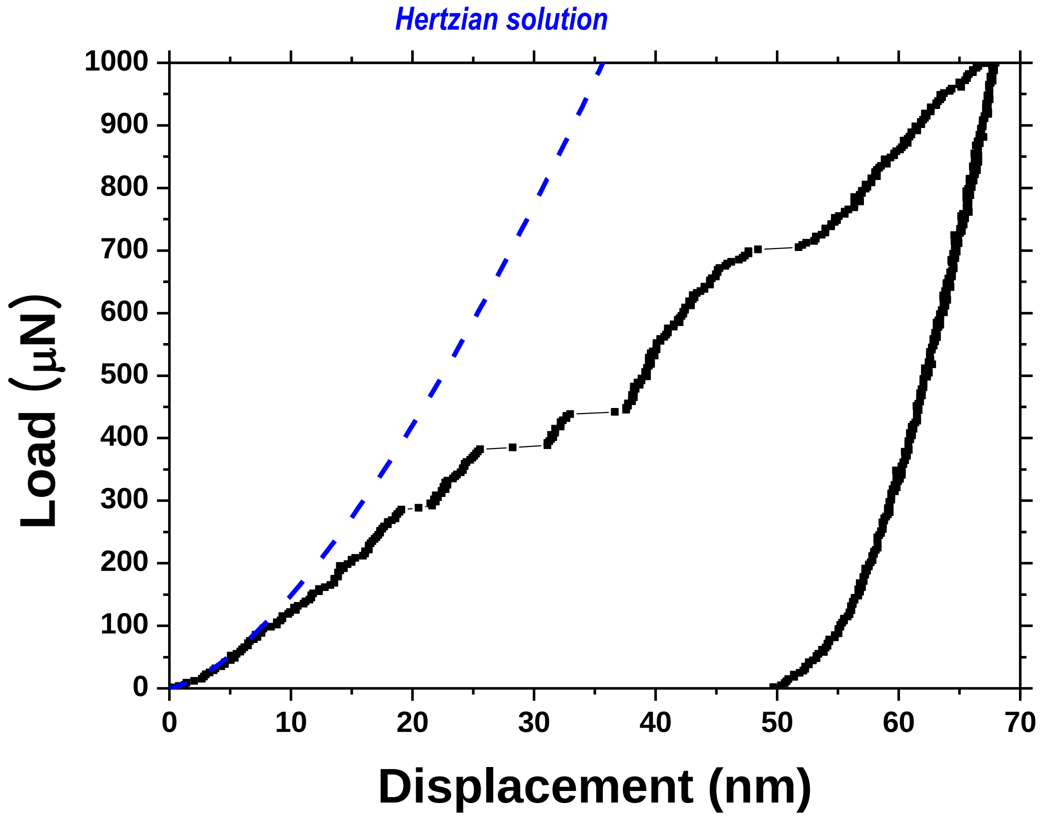

Pop-in Analysis (Austenite)

Multiple Martensite

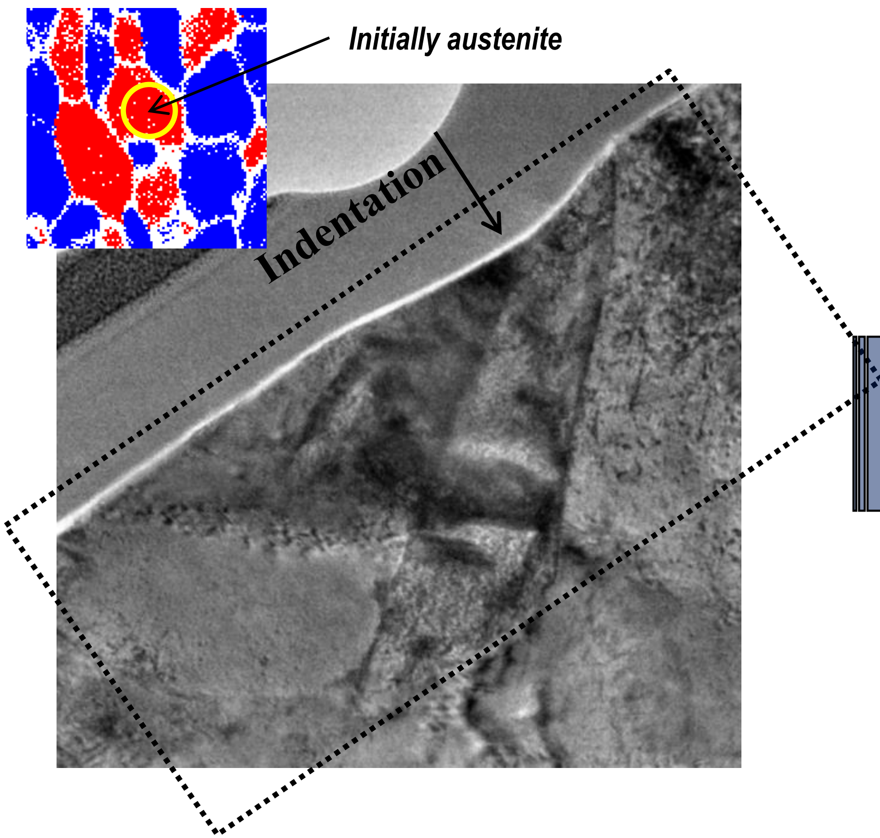

Automatic TEM mapping : A-STAR

Step size : 20nm

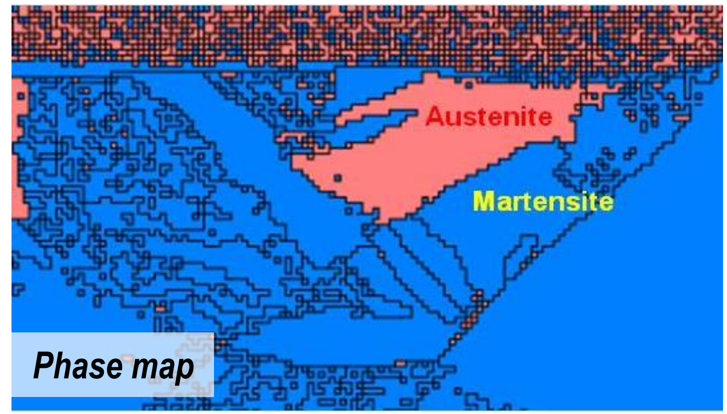

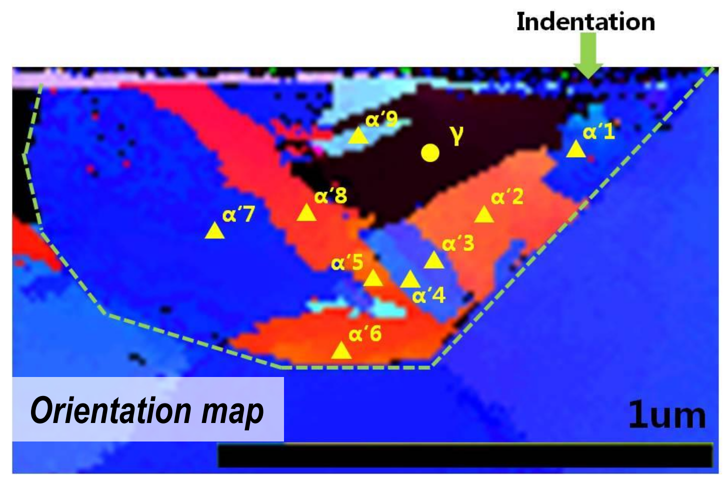

Pop-in Analysis (Austenite)

Variant selection

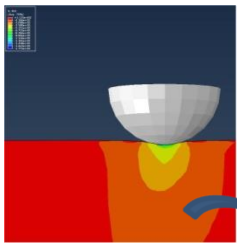

Stress distribution
by CP-FEM

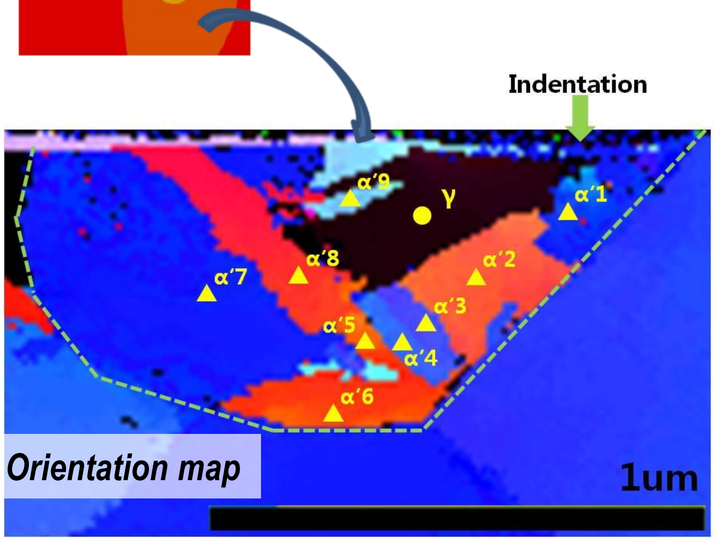

K-S relationship of each martensite

Position	Nearest K-S relationship **(Experimentally measured)**		Max. U_i **(Theory)**
	variant no.	misfit angle(°)	variant no.
α′1	**19**	5.55	1,2,**19**,20
α′2	20	3.72	15,16,23,24
α′3	21	1.06	15,16,23,24
α′4	22	0.85	15,16,23,24
α′5	**23**	2.40	15,16,**23**,24
α′6	**23**	1.67	15,16,**23**,24
α′7	14	4.03	15,16,23,24
α′8	13	1.81	15,16,23,24
α′9	**24**	3.61	15,16,23,**24**

Change of stress condition results in different K-S variants

γ→ε→α′ type TRIP steel

Material used

element	C	Mn	Si	Ni	N	Cr	Fe
wt.%	0.02	5.06	0.19	0.23	0.28	20.08	bal.

Phase map

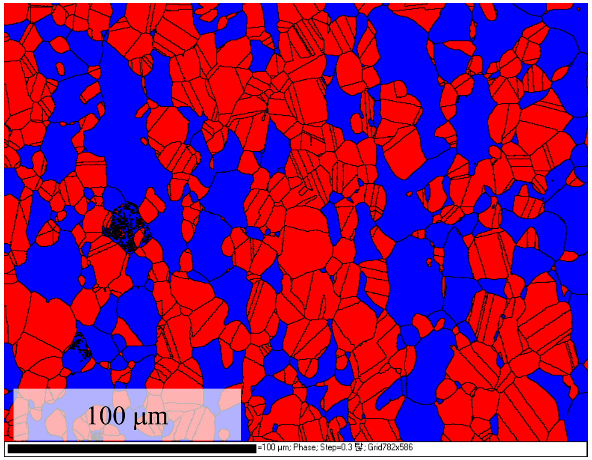

BCC (ferrite) FCC (Austenite)

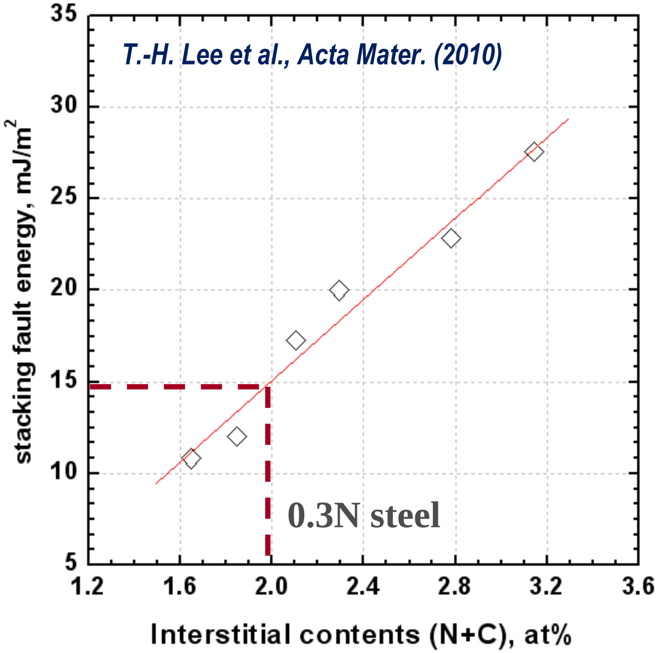

Predominating deformation mode in the early stage

: ε martensite formation

ε Martensite

Schematic description

ε martensite : stacking faults on $\{111\}_\gamma$ every two layers

*N.Bergeon et al., Mater.Sci.Eng.A (1997)

Lattice movement

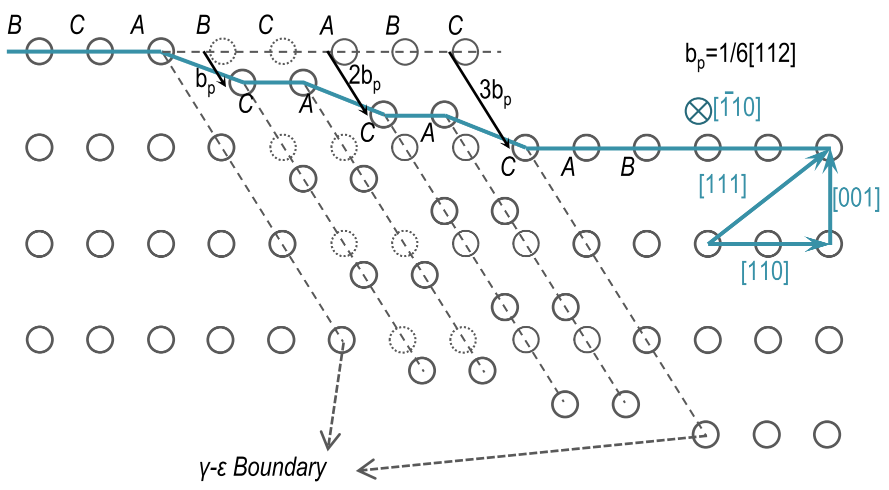

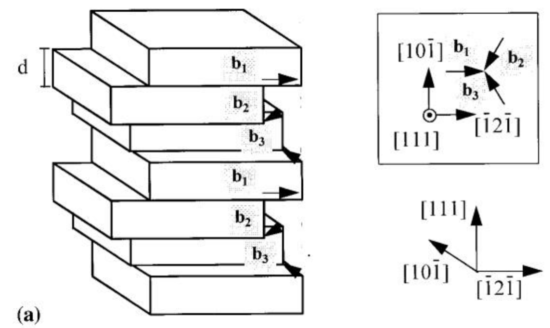

"Self-accomodated" stacking

: Thermal ε martensite

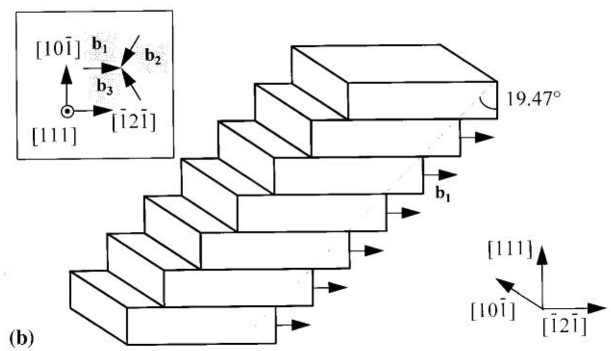

"Monopartial" stacking

: Stress-induced ε martensite

Shoji-Nishiyama orientation relation

$\{111\}_\gamma // \{0001\}_\varepsilon$, $<110>_\gamma // <11\text{-}20>_\varepsilon$

Deformation Microstructure

Tensile strained, TEM

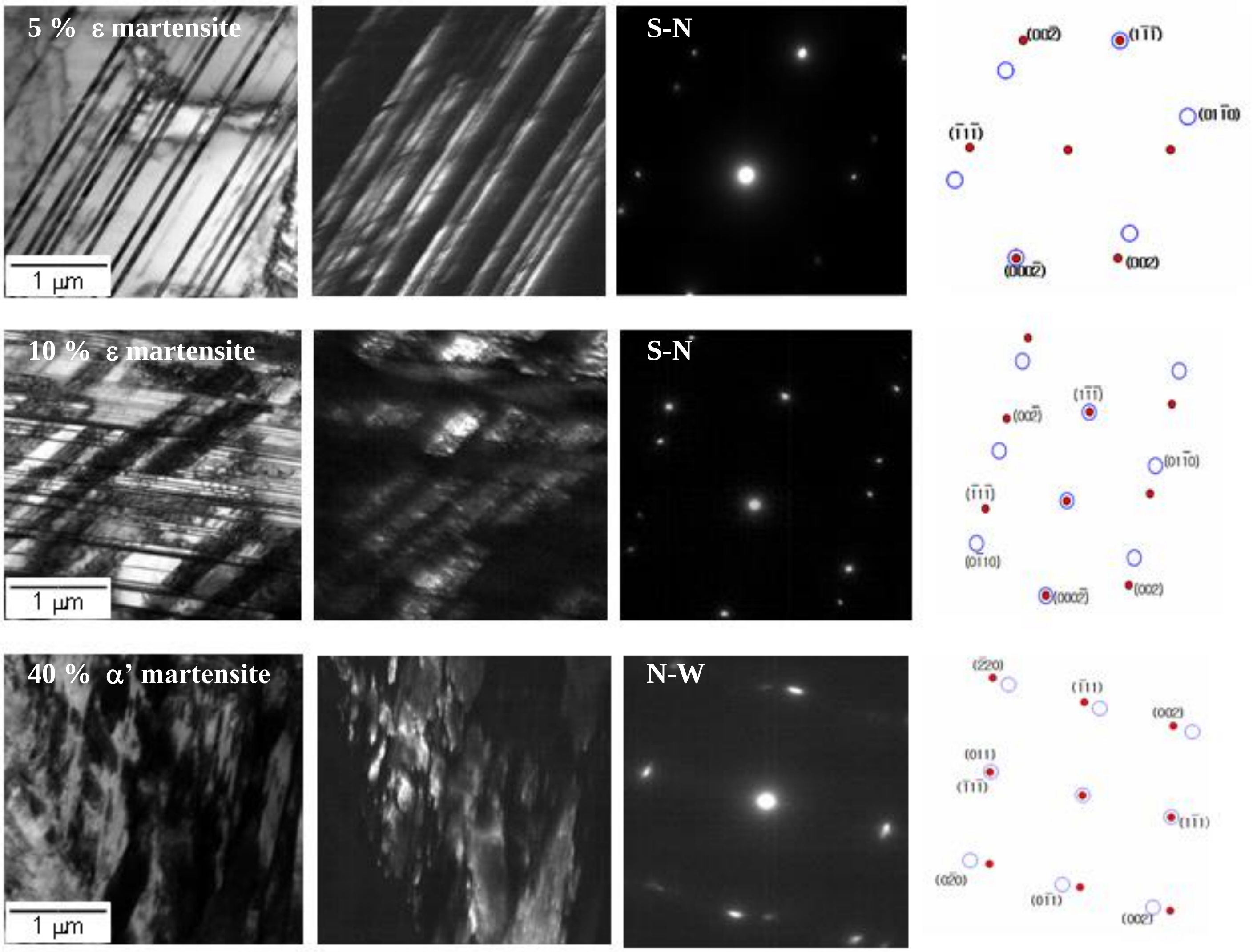

Results

Nanoindentation

Load-displacement Curve

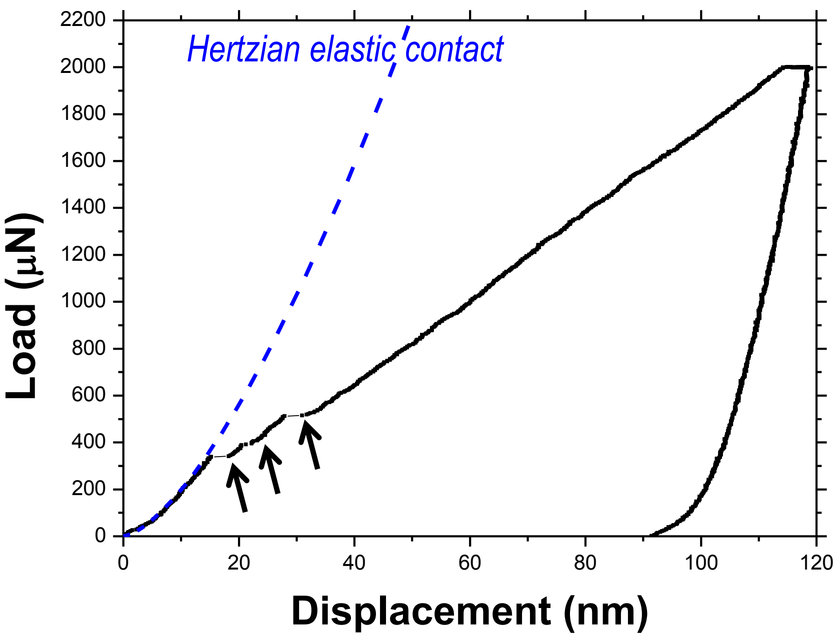

Stepwise pop-ins at yielding

EBSD phase map
(red : FCC, blue : BCC)

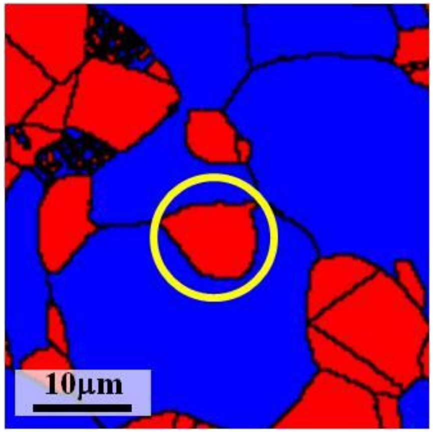

Orientation map (ND)

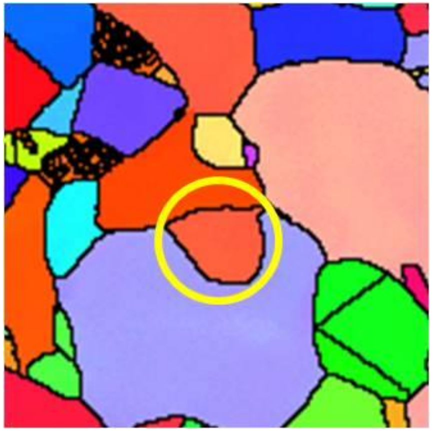

SPM

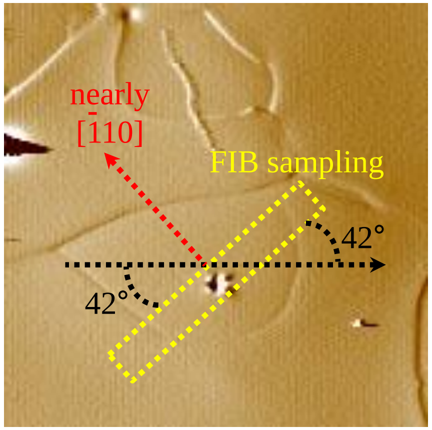

Cross-section

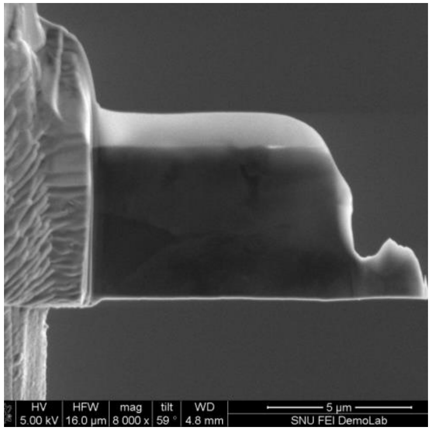

Results : Microstructure

TEM

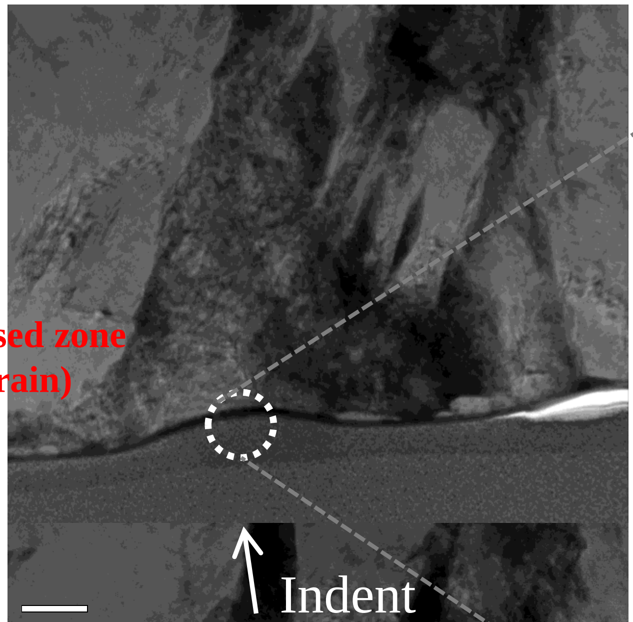

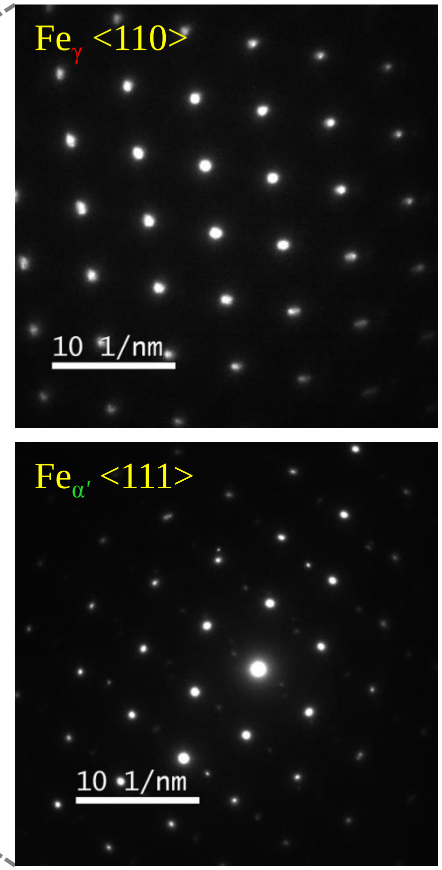

γ and α′ were found

➡ γ already had transformed to **α′**

Results : Microstructure

HR-TEM

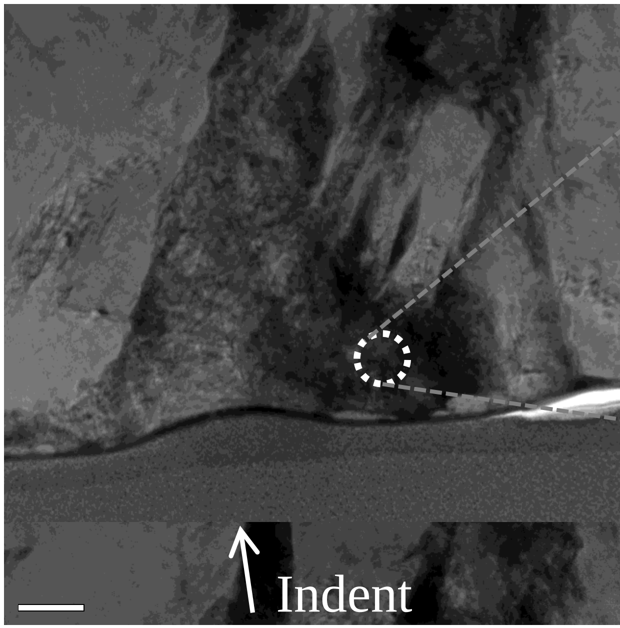

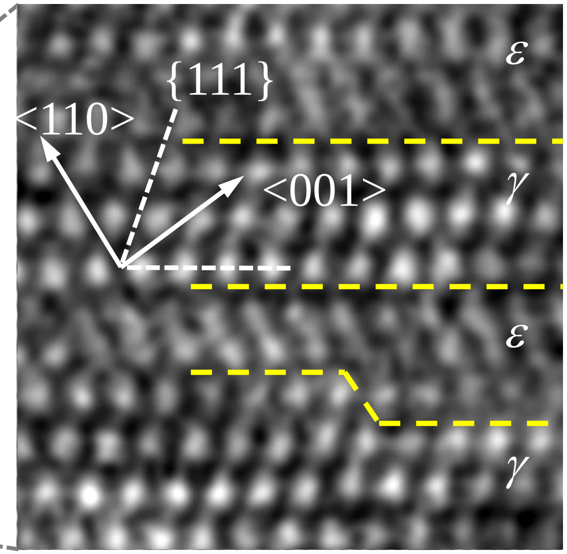

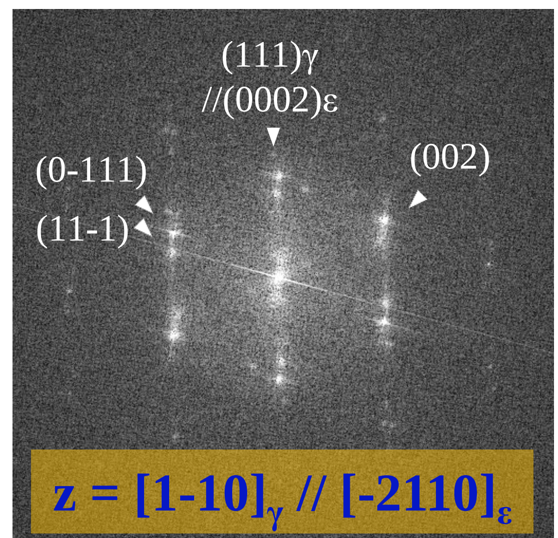

S-N orientation relationship

$(111)_\gamma//(0001)_\varepsilon$, $[1\text{-}10]_\gamma // [\text{-}2110]_\varepsilon$

Lattice displacement by γ→ε transformation

Schematic description

The displacement along <112>

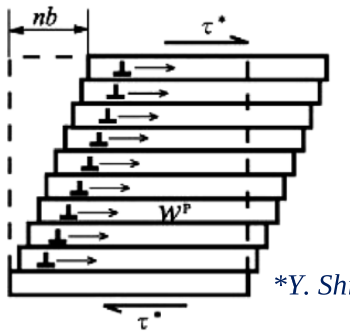

$$n|\mathbf{b}_\mathbf{p}| = \frac{na_\gamma}{\sqrt{6}}$$

* b_p = 0.13nm

*Y. Shibutani et al., Acta Mater. (2007)

Displacement along indentation axis

$$d_i = \frac{na_\gamma}{\sqrt{6}}|\cos\lambda|$$

n : number of partial dislocations

λ : angle between indentation axis and <112>

lattice displacement of 12 variants of partial slip

Slip Plane	Partial Direction	Schmid Factor	Unit Displacement
(111)	[11-2]	**-0.483**	0.082 nm
(111)	[1-21]	0.324	0.055 nm
(111)	[-211]	0.158	0.027 nm
(-111)	[1-12]	0.384	0.112 nm
(-111)	[12-1]	-0.090	0.026 nm
(-111)	[211]	0.294	0.086 nm
(-1-11)	[112]	0.315	0.122 nm
(-1-11)	[-121]	0.121	0.047 nm
(-1-11)	[2-11]	0.194	0.075 nm
(1-11)	[-112]	0.464	0.093 nm
(1-11)	[121]	0.381	0.076 nm
(1-11)	[21-1]	-0.083	0.017 nm

Consistent with EBSD-TEM result

✓ Displacement along indentation axis by one ε layer (1b_p)= 0.082(nm)

✓ Pop-in measured was 1.75nm~3.02nm (corresponds to 20b_p~37b_p)

Pop-in in Ferrite

Pop-in & Yield Drop

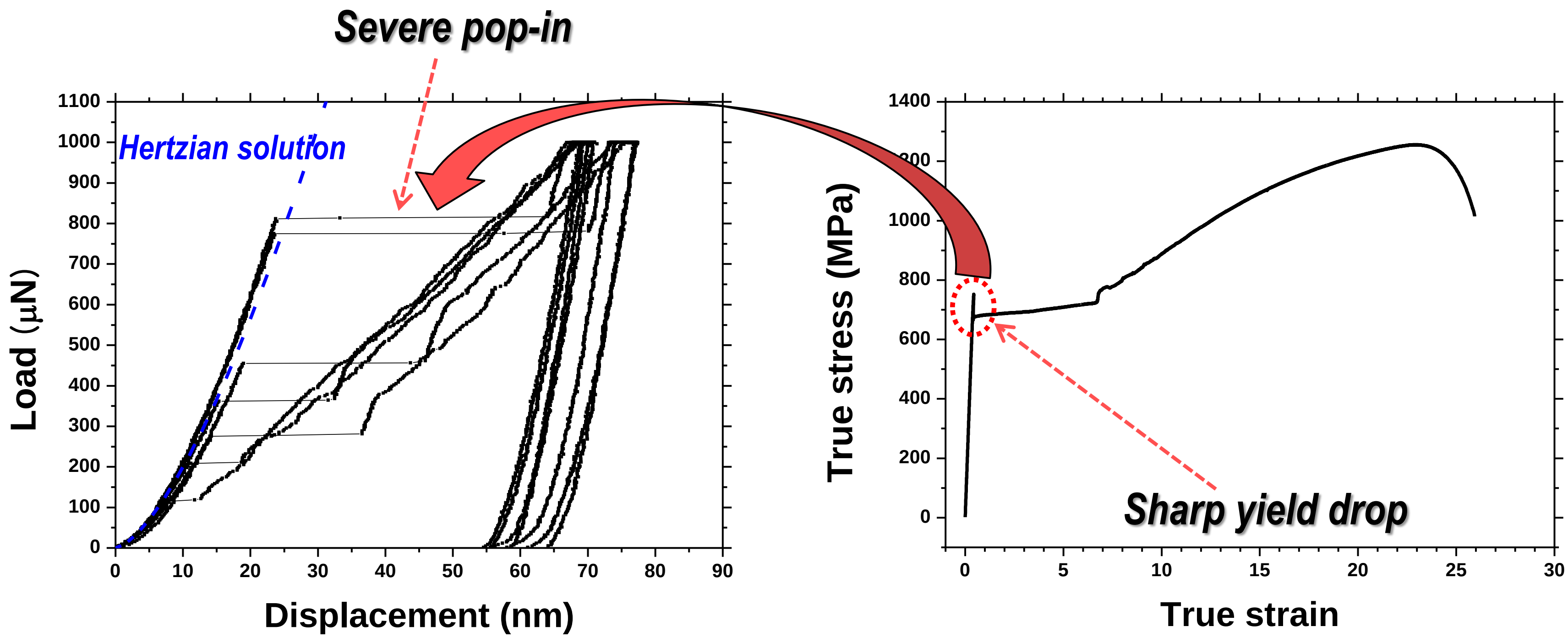

A much larger pop-in occurs at elastic-to-plastic transition

Sharp yield drop occurs at elastic-to-plastic transition

Why large pop-in? → **Pop-in ↔ Yield drop ?**

Material

Ferritic Steel

Chemistry

element	wt.%
C	0.06
Mn	0.16
Si	0.08
Al	0.02
N	0.0006
Cr	0.01
Fe	bal.

C, N : interstitial

Microstructure

(EBSD band contrast)

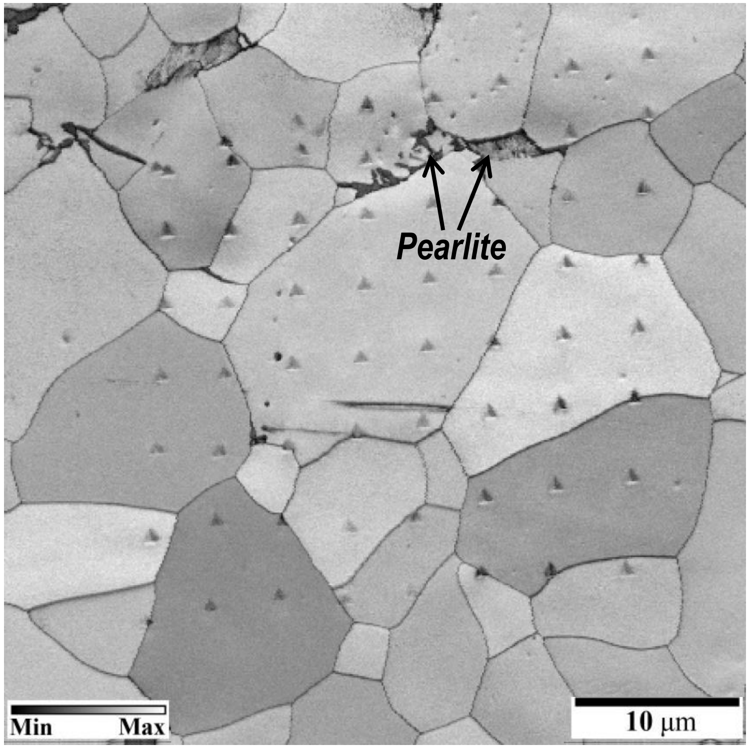

Ferrite : 99%
Pearlite : 1%

Tensile Behaviors

Yield Point Phenomenon

*T.-H. Ahn et al., J.Mater.Res., 27(1), 39-44 (2012)

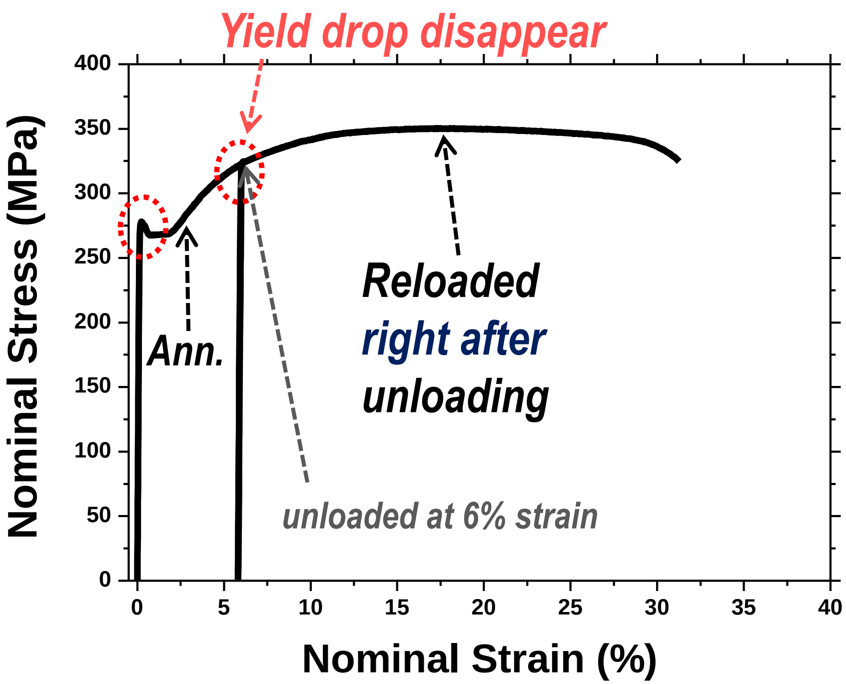

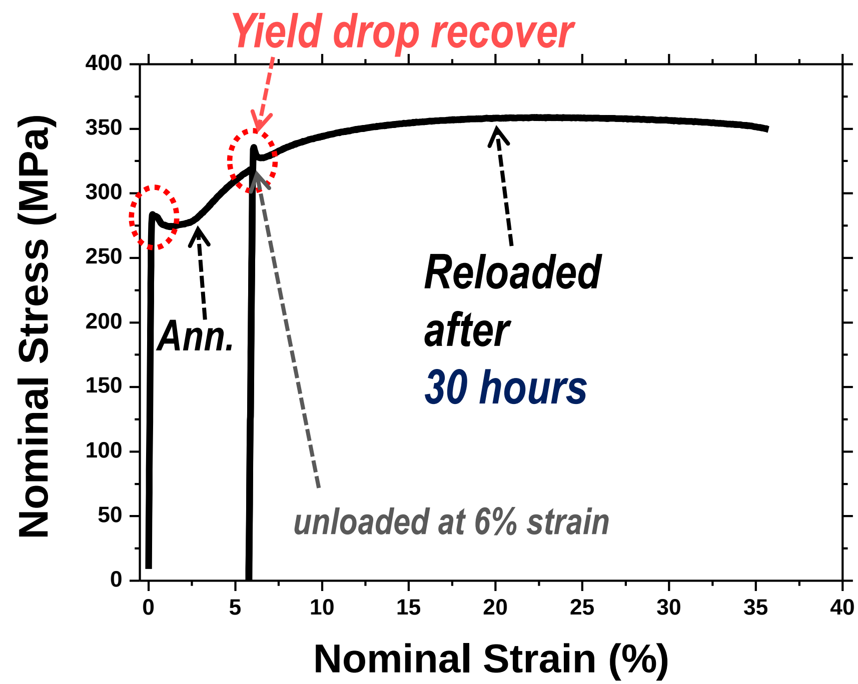

If pop-in in ferrite is related to yield drop,
analogous phenomenon must exist in the case of nanoindentation

Pop-in Behaviors (Ferrite)

Recovery of pop-in

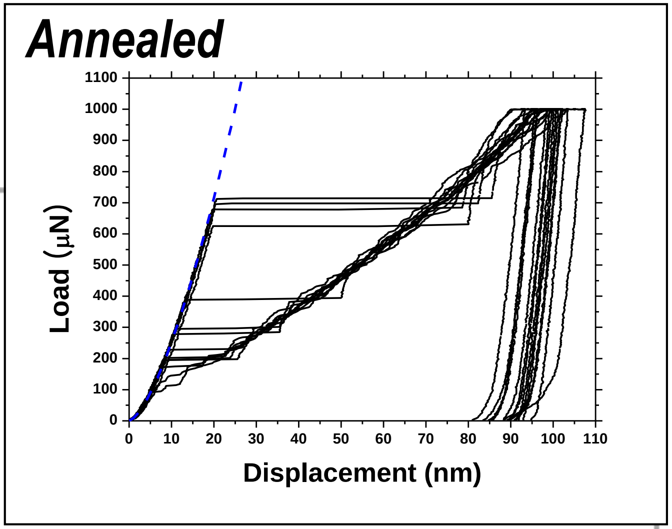

**T.-H. Ahn et al., J.Mater.Res., 27(1), 39-44 (2012)*

Pre-strained(6%) and strain aged at room temp.

Right after pre-strain → **30 hours later** → **3 weeks later**

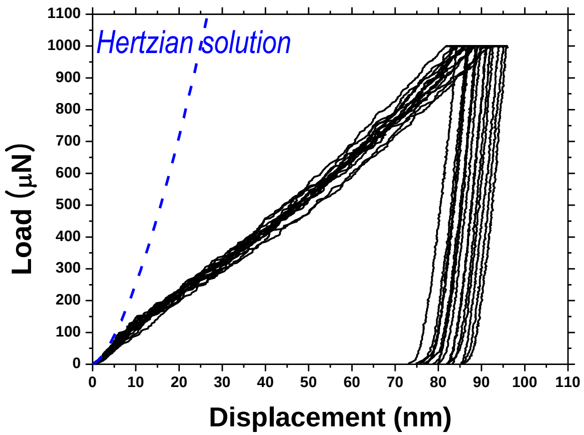

Pop-in disappeared

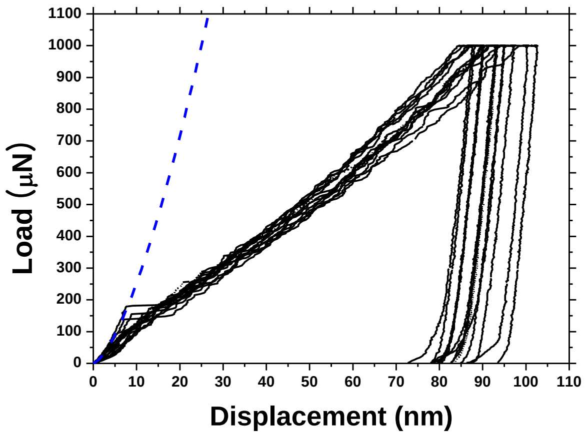

Pop-in reappeared

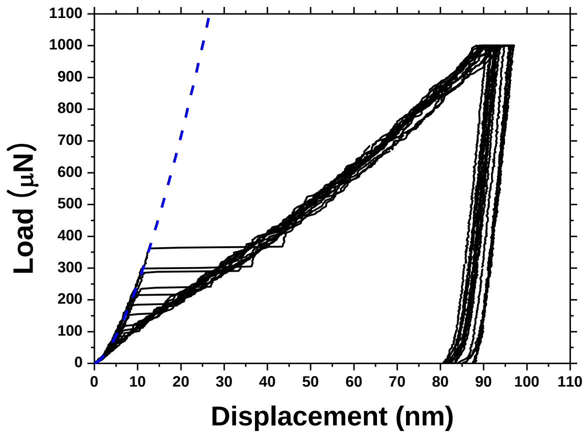

More frequent, larger pop-ins

Probability of pop-in increases with strain aging time

Summary

- ***The origin of nanoindentation pop-in behavior in steel was investigated.***
- ***Pop-in at elastic→plastic transition point (yielding) is likely the result of dislocation nucleation.***
- ***Austenite pop-in during plastic deformation was a result of geometrical softening by γ→α' phase transformation.***
- ***The ε-martensite formation in the early stage of plastic deformation possibly have contributed to pop-in.***
- ***Ferrite pop-in (nanoscale) was closely related to the sharp yield drop (macroscale).***

Strain by ε→α′ transformation

**α′ martensite was assumed to be BCC structure (c/a ratio was nearly 1 from TEM analysis)

Burgers' Mechanism

Burgers Orientation relation

$\{110\}_{bcc}//\{0001\}_{hcp}$, $<111>_{bcc}//<11\text{-}20>_{hcp}$

Transformation M

$[0001]_{hcp}$ → $[110]_{bcc}$
$[11\text{-}20]_{hcp}$ → ½ [111

Type	Net atom displacement	Contraction along Indentation axis
γ→ε	0.13nm (b_p)	-0.0824nm
ε→α′ (c-axis)	0.02nm	-0.0068nm

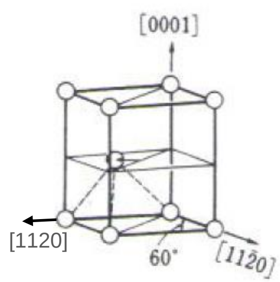

HCP

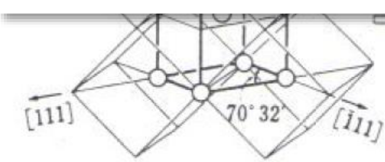

BCC

*W.G.Burgers, Physica (1934)

Strain in unit HCP crystal

c-axis ($[0001]_{hcp}$ → $[110]_{bcc}$)

$$|110|_{\alpha'} - |0001|_{\varepsilon} = \sqrt{2}a_{\alpha'} - \frac{2a_\gamma}{\sqrt{3}}c_\varepsilon$$

$$= 0.395nm - 0.416nm = -0.02nm$$

(Contracts 0.54% along c-axis)

→ ½<111>$_{bcc}$)

11] (sheared)

$$= a_{\alpha'} \cdot \cos(19.68°) - \frac{a_\gamma}{\sqrt{2}}$$

6nm = +0.04nm

(2) [1120]→½[111]

$$\frac{1}{2}|111|_{\alpha'} - |1120|_{\varepsilon} = \frac{\sqrt{3}a_\alpha}{2} - \frac{a_\gamma}{\sqrt{2}}$$

$$= 0.242nm - 0.226nm = +0.02nm$$

(Expands 23.9%(total) in a-axes)

*Lattice parameters were calculated from measured SADPs
$a_{\alpha'}$: Lattice parameter of α′ a_γ : Lattice parameter of γ

Insufficient lattice movements for pop-in